Distinct Ecological Adaptations and Habitat Responses to Future Climate Change in Three East and Southeast Asian Sapindus Species

Jiming Liu
Beijing Forestry University https://orcid.org/0000-0003-2926-8038
Yuanyuan Xu
Beijing Forestry University
Caowen Sun
Nanjing Forestry University
Xin Wang
Beijing Forestry University
Yulin Zheng
Beijing Forestry University
Shuanglong Shi
Beijing Forestry University
Zhong Chen
Beijing Forestry University
Qiuyang He
China Jiliang University
Xuehuang Weng
Yuanhua Forestry Biological Technology Co., Ltd.
Liming Jia (jlm@bjfu.edu.cn)
Beijing Forestry University

Research

Keywords: Sapindus, MaxEnt model, conservation, habitat distribution, Climate change, ecological niche model

Posted Date: May 4th, 2021

DOI: https://doi.org/10.21203/rs.3.rs-438835/v1

Abstract

Background: *Sapindus* is an important biodiesel, biomedical, and multifunctional economic forest species in Asia, however its germplasms have been persistently damaged or lost. It is imperative to conserve the diversity of *Sapindus*. This study aimed to reveal the potential habitat distribution patterns of *Sapindus mukorossi*, *Sapindus delavayi*, and *Sapindus rarak* in response to current environment and future climate change, and identify hotspots of habitat degradation/expansion to facilitate climate change-adaptive biological conservation.

Methods: Using current environmental data and future climate projections (2021–2100), we simulated the present and potential future habitats of *Sapindus mukorossi*, *Sapindus delavayi*, and *Sapindus rarak* in east and southeast Asia using a maximum entropy (MaxEnt) model that was developed based on 2041 occurrence records.

Results: The model showed that precipitation may play an important role in framing the potential habitats of *Sapindus*; however, *S. delavayi* was more sensitive to minimum temperatures (-2 °C to 3 °C) and elevation (1200-2000 m), while *S. rarak* was more demanding in terms of solar radiation (annual mean Uvb of 4600 to 5000 J/m^2/day). Under the current environment, *S. mukorossi* has the widest suitable habitat distribution (250.24 × 10^4 km^2), followed by that of *S. rarak* (173.49 × 10^4 km^2), and *S. delavayi* (78.85 × 10^4 km^2). Under future climate change scenarios, the habitat distribution of *S. mukorossi* will expand and contract, that of *S. delavayi* exhibited significant expansion. In contrast, future *S. rarak* habitat distribution exhibited significant contraction.

Conclusions: There were significantly distinct ecological adaptations among *Sapindus mukorossi*, *Sapindus delavayi*, and *Sapindus rarak* in east and southeast Asia. The contraction areas should be subject to germplasm collection and ex situ conservation preferentially. The modelled unchanged areas should be used for potential future *Sapindus mukorossi*, *Sapindus delavayi*, and *Sapindus rarak* conservation and utilization.

1. Background

Humans have a significant influence on future climate change, primarily reflected in the generation of anthropogenic greenhouse gas emissions (Neukom, Barboza, Erb, Feng, & Gunten, 2019; T. F. Stocker et al., 2013). The Intergovernmental Panel on Climate Change (IPCC) estimates that greenhouse gas emissions will result in a decadal 0.2°C global average temperature increase, and global temperatures will rise by, at most 2.64.8°C, and at least 0.3–1.7°C in the 21st century (T. F Stocker et al., 2014). The resulting variations in extreme temperature and precipitation patterns threaten the stability and diversity of forest ecosystems globally (Eastman, Florencia, Elia, John, & Assaf, 2013; Y. Liu, Yan, Li, & Motesharrei, 2015). The extinction rate of species will subsequently increase, and warmer temperatures may affect plant growth and yield (Hatfield & Prueger, 2015; Lawler, 2009; Ray, Gururaja, & Ramchandra, 2011). The Earth has experienced several climatic upheavals, and plants tend to alter their bioecological characteristics, phenology, or resilience response mechanisms through natural selection and genetic evolution to gradually spread or migrate to more suitable habitats to avoid being affected by adverse climatic conditions (R. T. Corlett & Westcott, 2013; Hewitt, 2000; Thomas et al., 2003). However, in the face of rapid climate change, it is unrealistic for plants to evolve adaptation strategies in such a short period, especially for arbour species. Therefore, exploring the potential habitat distributions of cherished species under future climate change is crucial to their diversity and conservation.

Sapindus is an evergreen, or deciduous, tree in the Sapindaceae family, which comprises 13 species with a global distribution in warm-temperate to tropical regions, found mainly in southeast Asia and North and South America (J. Liu et al., 2017). Among these, *Sapindus mukorossi* (*S. mukorossi*), *Sapindus delavayi* (*S. delavayi*), and *Sapindus rarak* (*S. rarak*) are concentrated in east and southeast Asia (J. Liu et al., 2017). Owing to the high yield of its seed oil (26.69–44.69%), as well as the high medium-chain monounsaturated fatty acid content (Sun, Jia, Xi, Wang, & Weng, 2017), *Sapindus* seed oils are suitable for biodiesel production according to American Society for Testing and Materials (ASTM) D6751 and the European EN 14214 standards (Chakraborty & Baruah, 2013; Pelegrini et al., 2017; Sun et al., 2019). Crude extracts from the fruit pericarps of *Sapindus* are also rich in triterpenoid saponins (4.14–27.04%) and sesquiterpenoids (J. Liu et al., 2019; Xu, Jia, Chen, & Gao, 2018), particularly in *S. rarak*, which exhibit excellent surface activity as well as antibacterial (Basu, Basu, Bandyopadhyay, & Chowdhury, 2015), elution (Mukherjee, 2015; Mukhopadhyay, Hashim, Sahu, Yusoff, & Gupta, 2013; Mukhopadhyay et al., 2016), antibacterial (Shinobu-Mesquita et al., 2015; Smu?ek et al., 2016), insecticidal (Shinobu-Mesquita et al., 2015; Smu?ek et al., 2016), pharmacological (Rodriguez-Hernández, Demuner, Barbosa, Csuk, & Heller, 2015), and physiological (Singh & Singh, 2008) properties. Saponin serves as an efficient natural surfactant in commercial soaps, shampoos, and cosmetic cleansers (Muntaha & Khan, 2015), and the root and fruit of *Sapindus* trees are used in traditional Chinese medicine. Therefore, *Sapindus* is regarded as an important biodiesel, biomedical, and multifunctional economic forest species (J. Liu et al., 2017; Sun, Jia, Ye, Gao, & Weng, 2016). *Sapindus* germplasm resources are widely distributed; however, they are generally scattered in the form of single plants or extremely small populations. Further, with global deforestation and the rapid anthropogenic development, *Sapindus* germplasms have been persistently damaged or lost in recent decades, especially in China, India, and Nepal (Jia and Sun, 2012; Liu et al., 2017). We doubt that *Sapindus* will experience a greater loss of diversity under future climate change. It is imperative to conserve the diversity of *Sapindus*, and natural populations at risk of destruction should be protected through in or ex situ conservation. However, there is the question of where *Sapindus* germplasm collection should be prioritised: where should the germplasms we have collected be preserved and cultivated under current environment and future climate change? Further, how should we preserve and cultivate different *Sapindus* germplasm species?

Zhang et al. (Zhang, Jing, Li, Liu, & Fang, 2019) and Peng et al. (Peng et al., 2019) explored suitable habitats for *Cinnamomum camphora* and *Paeonia ostia* under current and future climate conditions, respectively, using ecological niche models and offered suggestions for their respective targeted collection and preservation. Ashish (Pal, Vaishnav, Meena, Pandey, & Singh, 2020) also simulated the adaptability and limiting factors of *Sapindus emarginatus* Vahl in the face of future climate regimes through two ecological niche models. Therefore, ecological niche model appear one of the optimal solutions to establishing how species will adapt to future climate scenarios. Plant niches are habitats with a minimum threshold necessary for a plant's survival (Barry, Moore, & Cox, 1980). The forest niche is strongly affected by the environment, and its niche changes or moves with environmental changes. The principle of ecological niche models is to infer the ecological needs of species through mathematical models based on occurrence data and environmental factors to draw a statistical or

mechanistic model of their potential distributions (Araújo & Peterson, 2012; Elith & Leathwick, 2009; Zhu, Liu, Bu, & Gao, 2013). Benefitting from the simplicity of niche models and data accessibility (Merow et al., 2014), researchers can often estimate the potential habitat distribution and range shifts of species under future climate change. At present, the most commonly used niche models are the GARP (Stockwell, 1999), MaxEnt (Elith et al., 2006), Bioclim (Beaumont, 2005), random forest (Cutler et al., 2007), and boosted regression tree (Elith, 2008) models. Many model intercomparison studies have reported that the MaxEnt model, which is based on the principle of maximum entropy (Elith & Leathwick, 2009; Elith et al., 2011; Steven J. Phillips, Anderson, & Schapire, 2006), typically outperforms other species distribution models (SDMs) in terms of high tolerance and high predictive accuracy (Li, Du, & Wen, 2016; Merow et al., 2014; Merow, Smith, & Silander, 2013). Over the past decade, research teams have achieved rich results in the study of rare animal and plant diversity protection (Guo, Guo, Shen, Wang, & Wang, 2019; Huang et al., 2019; Rong et al., 2019; W. Wang et al., 2019), invasive species risk prediction (Ramos, Kumar, Shabani, & Picanco, 2019; Sultana, Baumgartner, Dominiak, Royer, & Beaumont, 2020), marine ecosystem protection (Melo-Merino, Reyes-Bonilla, & Lira-Noriega, 2020; Sterne, Retchless, Allee, & Highfield, 2020), disaster distribution prediction (Convertino, Annis, & Nardi, 2019), and disease propagation (Ardestani & Mokhtari, 2020; Hanafi-Bojd, Vatandoost, & Yaghoobi-Ershadi, 2020) using the MaxEnt model. However, *S. mukorossi* is the most widely distributed species of *Sapindus* in Asia, and thus far, there are no reports exploring its habitat distribution using ecological niche models. Adopting ecological niche models to explore the distribution of *Sapindus* habitat distribution and their responses to future climate change is likely an effective strategy to address the conservation of *Sapindus* germplasm diversity.

In this study, we combined principal component analysis, the MaxEnt model, and ArcGIS for the three major *Sapindus* species in east and southeast Asia, namely, *S. mukorossi*, *S. delavayi*, and *S. rarak*. Based on 2,041 occurrence records, we drove models using current climate normals (averages between 1970 and 2000) and future climate projections (averages between 2021 and 2100) to investigate the habitat distribution and centroid shifts of *S. mukorossi, S. delavayi*, and *S. rarak*. The three objectives for this study were as follows: (1) to determine the spatial heterogeneity of the distribution of *S. mukorossi*, *S. delavayi*, and *S. rarak*; (2) to project suitable habitats for these three *Sapindus* species under current environmental conditions; and (3) to reveal the potential habitat redistribution patterns of these three *Sapindus* in response to future climate change, and identify hotspots of habitat degradation/expansion to facilitate climate change-adaptive biological conservation.

2. Methods

2.1 Study area

Our study area was located in east and southeast Asia, the natural range of *S. mukorossi*, *S. delavayi*, and *S. rarak*, which comprises 15 countries, including China, Afghanistan, Myanmar, Vietnam, Brunei, Cambodia, Indonesia, Malaysia, the Philippines, Japan, North Korea, and South Korea. The study area covered an area of 14,770,700 square kilometres, lying between 40°N latitude and 10°N latitude and between 90°E and 150°E longitude, and could be divided into climate zones of subtropical monsoon, temperate monsoon, tropical rainforest, and tropical monsoon. The annual mean temperature fluctuated from 3.82°C in the Qinghai-Tibet Plateau to 27.60°C in the tropical region, and annual precipitation varied from 608 mm in the Qinghai-Tibet Plateau to 3685 mm in Indonesia, with elevations ranging from 1 to 3817 m.

2.2 Model building

2.2.1 Occurrence records

We collected 2041 occurrence records from well-planned surveys (Fig. 1), including (1) 225 occurrence records from field germplasm surveys of *S. mukorossi*, *S. delavayi*, and *S. rarak* in China; (2) 21 occurrence records from the Chinese National Plant Specimen Resource Center (CVH, http://www.cvh.ac.cn/), (3) 1772 occurrence records from the Global Biodiversity Information Facility (GBIF, https://www.gbif.org/), and (4) 23 occurrence records from the Chinese National Specimen Information Infrastructure (NSII, http://www.nsii.org.cn/2017/). In total, the occurrence records included 1849 accessions of *S. mukorossi*, 109 accessions of *S. delavayi*, and 83 accessions of *S. rarak* (Table S1).

There were some spatial clusters of occurrence records, particularly in China, Vietnam, and Japan. When such spatial clusters of occurrence exist, models often overfit environmental biases and inflate model performance values (Veloz 2009; Hijimans et al. 2012; Boria et al. 2014). Therefore, we employed the spatially rated occurrence data tool of SDMtoolbox 2.0, and set the spatial interval to 10 km to eliminate spatial occurrence clusters. The elimination resulted in 419 occurrence records, which were subsequently employed in the models, which included 342 *S. mukorossi*, 41 *S. delavayi*, and 36 *S. rarak* occurrence records.

2.2.2 Environmental factors

In total, 32 environmental factors were applied to the projection, including bioclimatic, topographical, UV-radiation, and soil parameters, to model potential suitable habitat for *Sapindus* (Table 1). The bioclimatic factors for current climate conditions were extracted from the 2.5 min resolution historical climate (averages for 1970–2000) database (https://www.worldclim.org/data/worldclim21.html). Topographical factors were obtained from the WorldClim dataset (https://www.worldclim.org/data/worldclim21.html). Soil factors were extracted from the Centre for Sustainability and the Global Environment dataset (https://nelson.wisc.edu/sage/). UV radiation variables were obtained from the glUV dataset (https://www.ufz.de/gluv/) (Beckmann et al., 2014).

Table 1
Environmental factors used in this study and their respective codes.

Data type	Code	Environmental factor
Bioclimatic factor	Bio1	Annual mean temperature
	Bio2	Mean diurnal range
	Bio3	Isothermality
	Bio4	Temperature seasonality
	Bio5	Max temperature of warmest month
	Bio6	Min temperature of coldest month
	Bio7	Temperature annual range
	Bio8	Mean temperature of wettest quarter
	Bio9	Mean temperature of driest quarter
	Bio10	Mean temperature of warmest quarter
	Bio11	Mean temperature of coldest quarter
	Bio12	Annual precipitation
	Bio13	Precipitation of wettest month
	Bio14	Precipitation of driest month
	Bio15	Precipitation seasonality
	Bio16	Precipitation of wettest quarter
	Bio17	Precipitation of driest quarter
	Bio18	Precipitation of warmest quarter
	Bio19	Precipitation of coldest quarter
	Eva	Evapotranspiration
	Gdd	Growing Degree Days
	Sd	Snow Depth
Topography factor	Elv	Elevation
Soil factor	Npp	Net Primary Productivity
	Sm	Soil Moisture
	Soc	Soil Organic Carbon
	Sph	Soil pH
	Ar	Annual Runoff
UV-radiation variables	AmUV	Annual mean UVb
	SeaUV	Seasonality UVb
	HighUV	Highest UVb
	LowUV	Lowest UVb

Future climate projections were extracted from the 2.5 minute resolution shared socioeconomic pathways (SSPs) scenarios from the BCC-CSM2-MR global climate (2021–2040, 241–2060, 2061–2080, 2081–2100) database of Coupled Model Intercomparison Project 6 (CMIP6) (https://www.worldclim.org/), which included the SSP1-2.6 scenario (SSP126), SSP2-4.5 scenario (SSP245), SSP3-7.0 scenario (SSP370), and SSP5-8.5 scenario (SSP585) (Beckmann et al. 2014). These scenarios were employed into climate modelling and research to describe four possible future climates, all of which considered possible depending on the amount of greenhouse gases emitted in the near future. All environmental factors were statistically resampled to 2.5-minute resolution using ArcGIS.

2.2.3 Parameterization and model evaluation

The MaxEnt model utilises the maximum entropy principle, applying five different feature constraints (linear, product, hinge, quadratic, and threshold) to environmental variables to calculate the potential geographic distribution probability of species. We used the SDMtoolbox to carry out the MaxEnt model on the ArcGIS platform, with 25% of the occurrence data as testing data and 75% of the occurrence data as training data. To explore the key factors that shaped the habitat distribution of each species, we utilised a jackknife test with all model replications to rank the relative importance of the environmental factors, and

the response curves of each factor were visualised. To calibrate and validate the robustness of the MaxEnt model evaluation, receiver operating characteristic curve (ROC curve) analysis was conducted. An area under the receiver operating curve (AUC) was employed to estimate the accuracy of the model predictions (Steven J Phillips, 2008; Steven J. Phillips et al., 2006). Model performance was determined by the following criteria: poor (AUC < 0.8), good (AUC 0.90–0.95), and excellent (AUC > 0.95) (Araujo, Pearson, Thuiller, & Erhard, 2005; Guisan & Thuiller, 2005).

We converted the continuous suitability score (0–1) of the output of the MaxEnt model into a habitat distribution visualisation in ArcGIS. We reclassified the model suitability into four classes: unsuitable habitat (< 0.25), low suitability (0.25–0.50), suitable habitat (0.50–0.75), and high suitability (> 0.75).

2.2.4 Quantifying the magnitude and direction of habitat shifts

To quantify the magnitude of habitat distribution change in the projected distributions of each species under future climate scenarios, we compared the future habitat distributions to the initial distributions and classified pixels as (a) expansion, (b) unchanged, and (c) contraction (Brown, 2014). Subsequently, we calculated the expanded, unchanged, and contracted habitat areas under all future climate scenarios using ArcMap 10.5. Moreover, we calculated centroids for both current and future species distributions and employed these centroids to project a vector arrow to indicate the magnitude and direction of habitat shifts of each species using the SDMToolbox in ArcMap 10.5 (Brown, 2014).

2.3 Testing for Niche Divergence among *Sapindus* species

We used ArcMap 10.5 to obtain environmental factor data based on 32 environmental factor raster files for 419 occurrence data points from the three *Sapindus*. The species-level divergence associated with each of the environmental factors was examined using a nonparametric Kruskal–Wallis multiple-range test (Conover, 1980). Without a priori designation of species distribution, principal component analysis (PCA) was applied to the scaled data for the 32 environmental factors corresponding to all available occurrence data. The relative contribution of each environmental parameter to the formation of niche spaces was then illustrated using a PCA distance biplot (Hu et al., 2017). A nonparametric Kruskal–Wallis multiple-range test and PCA were implemented in the vegan and mvstats packages in R 3.6.3, respectively, and the biplots were constructed using a combination of the dvtools and ggplot packages in R 3.6.3.

3. Results

3.1 Niche Divergence of *S. mukorossi, S. delavayi*, and *S. rarak*

The niche divergence of *S. mukorossi, S. delavayi*, and *S. rarak* for each of the 32 environmental parameters were analysed by the nonparametric Kruskal-Wallis rank sum test, and revealed that three species of *Sapindus* showed a significantly distinct adaptability range to environmental variables when compared with each other ($p = 9.981e^{-14}$). The PCA of the 32 environmental factors identified four components that collectively explained 79.85% (PC1:39.44%, PC2:17.30%, PC3:13.58%, and PC4:9.55%) of the observed variation among the 419 occurrences (Fig. 2). Variables with the highest loading scores on PC1 were Bio17, Bio14, Bio6, and Bio9, which are closely associated with precipitation and temperature. PC2 correlated strongly with soil pH and elevation. PC3 was closely associated with soil nutrients, while PC4 was associated with the highest UVb and precipitation of the warmest quarter. The 419 occurrences were clustered into three distinct environmental spaces in the Cartesian coordinates formed by the first two principal components, and the clustering correlated closely with the three *Sapindus* species.

S. mukorossi, S. delavayi, and *S. rarak* exhibited significantly different ecological adaptations. *S. mukorossi* was the most widely distributed tree species and showed broad suitability. Compared with that of *S. mukorossi*, the ecological adaptation of *S. delavayi* indicated that the species preferred higher altitudes, higher mean diurnal range, and higher UV radiation. *S. rarak* showed a wider range of altitude adaptations and exhibited a higher demand for UV radiation and minimum temperatures.

3.2 Habitat distribution and key environmental factors of *Sapindus* under the current environment

Suitable distribution modelling for the three *Sapindus* species performed better than random distribution modelling, with testing AUC values ranging from 0.944 to 0.983, indicating that the models performed excellently in predicting suitable habitats in the current environment. We found that the predicted current suitable habitat distributions matched well with the actual ranges of the *S. mukorossi, S. delavayi*, and *S. rarak*, with overlaps found in the margins of neighbouring species distribution zones, such as in Guizhou Province, Sichuan Province, and Yunnan Province in China (J. Liu et al., 2019; Sun et al., 2018) .

3.2.1 Habitat distribution and key environmental factors of *S. mukorossi*

The MaxEnt model's internal jackknife test of factor importance showed that the precipitation of the warmest quarter (Bio18, 51.8 % of variation), isothermality (Bio 3, 18.9 % of variation), and net primary productivity (Npp, 15.6 % of variation) were the major contributors to the distribution model of *S. mukorossi*, with a cumulative contribution of 86.3% (Table 2). According to the MaxEnt results and environmental factor response curves, the ecological thresholds for the key environmental factors were 950–350 mm for the precipitation of the warmest quarter, 26–33 isothermality, and 1.02–1.08 kg/m^2 net primary productivity.

Table 2
Contributions of the key environmental factors in the MaxEnt models for *S. mukorossi*, *S. delavayi*, and *S. rarak*.

S. mukorossi				*S. delavayi*				*R.rarak*		
Variable	Environmental factor	Percent contribution (%)	Suitable threshold	Variable	Environmental factor	Percent contribution (%)	Suitable threshold	Variable	Environmental factor	Percent contribution (%)
Bio 18	Precipitation of warmest quarter	51.8	950–3500	Bio 18	Precipitation of warmest quarter	23.9	450–700	Npp	Net Primary Productivity	27.5
Bio 3	Isothermality	18.9	26–33	Npp	Net Primary Productivity	21.3	0.82–0.95	AmUV	Annual mean Uvb	15.1
Npp	Net Primary Productivity	15.6	1.02–1.08	Bio 6	Min temperature of coldest month	17	-2–3	Bio 13	Precipitation of wettest month	12.6
Bio 13	Precipitation of wettest month	4.1	500–1000	Bio 19	Precipitation of coldest quarter	10	50–80	Bio 18	Precipitation of warmest quarter	9.8
AmUV	Annual mean Uvb	3.4	-	Elv	Elevation	7.1	1200–2000	Bio3	Isothermality	9.6

The total habitat of *S. mukorossi* was 250.24 × 10^4 km^2, and mainly located in the Jiangxi Province, Guangdong Province, Guangxi Zhuang Autonomous Region, Hainan Province, Taiwan in southern China, and the Kinki, Shikoku and Kyushu regions in Japan and Vietnam (Fig. 3). The area of suitable habitat was 77.28 × 10^4 km^2, and the area of low suitability was 171.58 × 10^4 km^2, accounting for 30.88% and 68.57% of the total habitat area, respectively (Fig. 6). Areas of high suitability covered an area of only 1.38 × 10^4 km^2 (0.56%), concentrated in Hainan Province, local areas of Taiwan in China, and local areas in Japan.

3.2.2 Habitat distribution and key environmental factors of *S. delavayi*

The precipitation of the warmest quarter (Bio18, 23.9% variation; 450–700 mm), net primary productivity (Npp, 21.3% variation; 0.82 to 0.95 kg/m^2), minimum temperature of the coldest month (Bio 6, 17.0% variation; -2°C to 3°C), precipitation of the coldest quarter (Bio 19, 10.0% variation; 50–80 mm), and elevation (Elv, 7.1% variation; 1200–2000 m) were the major contributors to the distribution model of *S. delavayi*, with a cumulative contribution of 79.3% (Table 2).

The habitat distribution of *S. delavayi* was quite dissimilar to that of *S. mukorossi*. The habitat distribution of *S. delavayi* was highly concentrated in southwest China, with a total habitat area of 78.85 × 10^4 km^2 (31.51% of the habitat area of *S. mukorossi*) (Fig. 6). The areas of high suitability for *S. delavayi* were concentrated in the Sichuan Basin of the Sichuan Province, Kunming, Lijiang, Chuxiong, Qujing, and Zhaotong of Yunnan Province, and local areas in Linzhi City, Tibet, while areas of low suitability radiated to southern Shanxi Province, western Hubei Province, and local areas of the Guizhou, Henan, and Shandong Provinces (Fig. 4).

3.2.3 Habitat distribution and key environmental factors of *S. rarak*

For *S. rarak*, net primary productivity (Npp, 27.5% variation; 78–0.86 kg/m^2), annual mean Uvb (AmUV, 15.1% variation; 4600–5000 J/m^2/day), precipitation of the wettest month (Bio13, 12.6% variation; 310 to 550 mm), precipitation of the warmest quarter (Bio18, 9.8% variation; 600 to 2200 mm), and isothermality (Bio3, 9.6% variation; 49 to 55) were the major contributors to the distribution model, with a cumulative contribution of 74.6 % (Table 2).

The total suitable habitat area of *S. rarak* was 173.49 × 10^4 km^2 (Fig. 6), widely distributed in Yunnan Province in China, Myanmar, Thailand, Laos, Cambodia, Malaysia, Singapore, Indonesia, Philippines, Timor-Leste, and Papua New Guinea. Areas of high-suitability habitat covered only 8.28 × 10^4 km^2, with distribution predominantly in Lincang, Pu'er, and Xishuangbanna Dai Autonomous Prefecture in China's Yunnan Province, and local areas in eastern Myanmar, northern Thailand, and Indonesia (Fig. 5).

3.3 Potential distribution of three *Sapindus* species under future climate scenarios

By comparing the current suitable habitats (Fig. 3–5) with the projected suitable habitats from 2020 to 2100, we predicted the potential redistributions of *S. mukorossi*, *S. delavayi*, and *S. rarak* in response to 21st century climate change under four future climate scenarios (Fig. 7). The dynamics of the potential habitat areas of these three species exhibited different trends during the 21st century. Generally, our projections indicated that all species significantly differed in their habitat changes among the SSP126, SSP245, SSP370, and SSP585 scenarios, with some species dramatically expanding or contracting their habitat distributions.

Under the SSP126, SSP245, SSP370, and SSP585 scenarios, by 2100, the suitable habitat distribution of *S. mukorossi* showed a significant expansion toward higher latitudes and contraction in lower latitudes, with expansion occurring predominantly in the Sichuan Basin, Hubei Province, Hunan Province in China, and localised in southern Korea, and contraction occurring in Chongqing, Guangxi Zhuang Autonomous Region, Fujian Province, and Hunan Province in China (Fig. 7). The area of habitat expansion for *S. mukorossi* ranged from 7.13 × 10^4 km^2 (SSP370-2061-2080) to 14.28 × 10^4 km^2 (SSP585-2061-2080), while the areas of contraction ranged from 6.75 × 10^4 km^2 (SSP585-2041-2060) to 13.45 × 10^4 km^2 (SSP126-2041-2060) (Fig. 7; Figure S1). Unlike that of *S. mukorossi*, the projected suitable habitat distribution of *S. delavayi* underwent significant expansion and less pronounced contraction. The area of habitat expansion ranged from 12.51 × 10^4 km^2 (SSP585-2081-2100) to 18.02 × 10^4 km^2 (SSP245-2061-2080), mainly occurring in Sichuan Province, Yunnan Province, and Guizhou Province in China, while the area of contraction ranged from 5.56 × 10^4 km^2 (SSP245-2041-2060) to 7.53 × 10^4 km^2 (SSP370-2081-2100), and mainly

occurred to Tibet, and only slightly occurred in the periphery of the Sichuan Basin (Fig. 7; Figure S2). In contrast, the projected suitable habitat distribution of *S. rarak* underwent significant contraction and minor expansion. During 21st century (present day to 2100), the areas of suitable habitat distribution for *S. rarak* contracted from 42.73×10^4 km^2 to 72.30×10^4 km^2, mainly in the northern Yunnan Province in China, eastern Myanmar, Thailand, Cambodia, Malaysia, Indonesia, and the Philippines (Fig. 7; Figure S3). These changes were predicted to be more intensive under the SSP370 and SSP585 scenarios than under the SSP126 and SSP245 scenarios (Fig. 7; Figure S3). Furthermore, climate change was predicted cause an expansion from 18.73×10^4 km^2 to 51.23×10^4 km^2 of suitable *S. rarak* habitat distribution in Mizoram and Manipur in India, northern Myanmar, Indonesia, and the Philippines (Fig. 7).

3.4 Habitat and spatial centroid shifts in the 21st century

The vectors between the present and future centroids indicated that the magnitudes and directions of the range shifts of these *S. mukorossi, S. delavayi*, and *S. rarak* differed under different future climate scenarios (Fig. 8). The geographical centroid of the potential habitat of *S. mukorossi* in the current scenario was currently located at 113.74°E, 27.64°N, in Liling County, Hunan Province, China (Fig. 8A). *S. mukorossi* was predicted to shift its centroid to the east and south under all emission scenarios. Under the SSP126 and SSP245 scenarios, the centroid was predicted to shift eastward by the mid-21st century and then shift southward by the late 21st century. The centroid generally shifted farther eastward under the SSP370 and SSP585 scenarios, with the farthest shift eastward to Luxi County, Jiangxi Province, China (located at 113.97°E, 27.70°N) under the SSP585 scenario.

The geographical centroid of the potential habitat of *S. delavayi* in the current scenario was currently located at 103.09°E, 27.83°N, in the southern Liangshan Yi Autonomous Prefecture, Sichuan Province, China (Fig. 8B). The centroid of *S. delavayi* was predicted to shift south-eastwards under all future climate scenarios, from the present position towards Zhaotong city, Yunnan Province, China, with a maximum distance to Yiliang county, Yunnan Province, China (located at 104.20°E, 27.73°N).

Shifts that are more complex were predicted for in *S. rarak*, which was predicted to shift its centroid to the northwest under the SSP126 and SSP245 climate scenarios but to the southeast under the SSP370 and SSP585 climate scenarios. The centroid of *S. rarak* was predicted to shift from Udon Thani, Thailand (located at 103.24°E, 16.93°N) to the north of Udon Thani, Thailand (located at 102.09°E, 17.77°N) under the SSP126 scenario, while it shifted to the Maha Sarakham, Thailand (103.27°E, 16.10°N) under the SSP370 scenario (Fig. 8C).

4. Discussion

This study projected the current and future potential suitable habitats for three *Sapindus* species in east and southeast Asia using the MaxEnt model based on occurrence data sets with mean AUCs of 0.964 and 0.959 for current and future models, respectively. Therefore, we believe that our model performance is robust and adequate for construing the overall suitable habitat distribution of *Sapindus*. To the best of our knowledge, this is the first study to analyse the suitable habitat distribution of *S. mukorossi*, *S. delavayi*, and *S. rarak* for the present and future using MaxEnt model.

4.1 Habitat distributions of *S. mukorossi*, *S. delavayi*, and *S. rarak* under the current environment

Sapindus is an ancient and widely distributed species; Engler (A. Engler, Melchior, & Werdermann, 1989) and Taylor (Taylor, 1990) found leaf fossils of *Sapindus* in Tertiary strata of North America. Xia (Xia, 1995) stated that *Sapindus* was widely distributed and highly differentiated from the Eocene to the Tertiary. Long periods of natural selection and geographical isolation have allowed *Sapindus* to differentiate and adapt in their respective regions, eventually forming their own unique environmental suitability and species-specific physiological tolerance. Liu (J. Liu et al., 2019) and Sun (Sun, Jia, et al., 2017; Sun et al., 2016) found considerable phenotypic variation in *S. mukorossi*, *S. delavayi*, and *S. rarak* when they investigated the germplasm resources of *Sapindus* in China. Wang (X. Wang, Liu, Rui, Xu, & Jia, 2020) found significant interspecific variation in leaf phenotypes between *S. mukorossi* and *S. delavayi* by observing the leaves of 117 *Sapindus* clones. Mahar (Kamalesh et al., 2011; Mahar, Meena, Rana, & Ranade, 2011; Mahar, Rana, Ranade, Pande, & Palni, 2013) revealed significant genetic divergences between populations of *S. mukorossi*, *S. trifoliatus*, and *S. emarginatus* by DNA molecular markers. Previous studies have demonstrated significant phenotypic and genetic variations between species and populations of *Sapindus*; however, little research has been reported on the ecological adaptations of *Sapindus*.

In this study, we demonstrated that there were significant variations in the ecological suitability among *S. mukorossi*, *S. delavayi*, and *S. rarak* through PCA and Kruskal–Wallis multiple-range tests. The MaxEnt model results indicated that precipitation and net primary productivity were common key environmental factors affecting the distribution of *S. mukorossi*, *S. delavayi*, and *S. rarak* (Table 2). Therefore, we suggest that precipitation and net primary productivity are essential requirements for the survival of *Sapindus*. However, when accounting for additional factors, apparent differences exist in the importance of elevation, minimum temperature, and solar radiation between *S. mukorossi*, *S. delavayi*, and *S. rarak*. Minimum temperature (-2°C to 3°C) and elevation (1200–2000 m) were the secondary critical environmental factors in determining the suitable habitat distribution of *S. delavayi*, and solar radiation (annual mean Uvb ranged between 4600 and 5000 J/m^2/day) was the secondary critical environmental factor for *S. rarak* (Table 2). The results of the biplot (Fig. 2) in the PCA supported these findings. Based on the genetic structure and geographical variation of *Sapindus* germplasms, Sun (Sun et al., 2018) found that areas of high altitudes and low minimum temperatures are suitable for the growth of *S. delavayi*. Ashish Kumar Pal (Pal et al., 2020) found that maximum temperature and annual precipitation were the most critical environmental factors determining the distribution of suitable habitats for *S. emarginatus* through the MaxEnt model. These findings also demonstrate that precipitation is a prerequisite for suitable habitat distribution of *Sapindus*, and that *S. emarginatus* similarly diverges into significantly different ecological suitability.

Our study indicated that *S. mukorossi* exhibited the widest distribution of suitable habitats, followed by that of *S. rarak*, and *S. delavayi*, concentrated in the high-altitude areas of southwest China. Sun (Sun et al., 2016) and Cai (Cai et al., 2018) found that *S. delavayi* has larger seed kernels than *S. mukorossi* and, thus, more suitable for cultivation as a biodiesel species. Therefore, it is recommended that *S. delavayi* biodiesel forests should be developed in the Sichuan

and Yunnan Provinces in China. Suitable habitats of *S. mukorossi* were widely distributed throughout southern China, southern Korea, and southern Japan (Fig. 3), whereas the suitable habitat areas for *S. rarak* were widely distributed in tropical and subtropical regions. Sun (Sun, Jia, et al., 2017) found that *S. mukorossi* shows strong breeding potential, and Liu (J. Liu et al., 2019) found that *S. rarak* exhibits strong biochemical potential for saponins. Combined with the MaxEnt results from this study, we suggest that *S. mukorossi* could be developed and cultivated in the Fujian, Jiangxi, Guangdong, and Guangxi Provinces in China, and *S. rarak* could be cultivated in the Yunnan Province in China, Thailand, and Myanmar.

4.2 Response of suitable habitat distribution to future climate change

Climate is the most critical ecological factor for plants, and changes in plant distribution are the clearest and most direct responses to climate. Future climate change may substantially change the structure and function of terrestrial ecosystems, resulting in significant changes in the extent and distribution of biological habitats (Barry et al., 1980; Lawler, 2009). The results of this study indicate that *S. mukorossi*, *S. delavayi*, and *S. rarak* display significantly distinct ecological adaptations. Therefore, they are also predicted to exhibit dramatically divergent responses in the face of future climate change. The habitat distribution of *S. mukorossi* will expand and contract in future climate change, with a trend towards expansion at higher latitudes and contraction at lower latitudes, with the centroid moving mainly eastward and southward. We hypothesised that rising minimum temperatures and better water circulation at higher latitudes and mid-altitudes (Gao, Pan, & Zhang, 1991), caused by climate change, will allow *S. mukorossi* to expand into these areas. Clark (Clark & D., 2004) indicated that average temperature and rainfall were generally negatively correlated in the tropics, and de la Peña and Hughes stated (Pea & Hughes, 2007) that climate change will lead to more erratic rainfall patterns and unpredictable high temperature spells in the tropics. In the face of future climate change, extreme heat and erratic rainfall and drought at low latitudes will likely lead to localised areas that are no longer suitable for the distribution of *S. mukorossi*.

S. delavayi showed significantly different distribution trends in response to climate change compared to that of *S. mukorossi*. Benefiting from future climate change, a large number of currently unsuitable areas in Sichuan and Yunnan Provinces in China are predicted to potentially become suitable for *S. delavayi*, with the centroid shifting south-eastward (Fig. 7; Fig. 8). We speculate that increased precipitation caused *S. delavayi* to expand outward from its original habitats; however, elevation remains a key ecological factor in determining the habitat distribution of *S. delavayi* (Sun et al., 2018), which prevents *S. delavayi* from expanding to lower elevations.

Interestingly, *S. rarak* exhibited a significant contraction trend in distribution, mainly in the northern Yunnan Province in China, eastern Myanmar, Thailand, Cambodia, Malaysia, Indonesia, and the Philippines, with the most significant contraction occurring in the SSP370 and SSP585 climate scenarios (Fig. 7; Fig. 8). Tran and Vien (Tran & Vien, 2011) indicated that increasingly erratic and variable rainfall, higher temperatures, more intense extreme weather events, droughts, floods, and rising sea levels will occur in Vietnam as the climate changes. Due to the long coastline and low average elevation in southeast Asia, excessive temperatures and complex weather patterns in the future may result in large areas no longer being suitable for *S. rarak* habitat.

Jayasinghe and Prevéy also found a declining trend in the area of suitable habitats for *Camellia sinensis* (L.) O. Kuntze (Jayasinghe & Kumar, 2019) and huckleberry (Prevéy, Parker, Harrington, Lamb, & Proctor, 2020) with climate change, while an expanding trend in the highly suitable habitat area was found for *Xanthoceras sorbifolia* Bunge (He, Ning, Guo, & Wei, 2019). In this study, the habitats of *S. mukorossi, S. rarak*, and *S. delavayi* exhibited different trends under future climate change. We believe that these differences were the result of distinct ecological adaptations among *S. mukorossi, S. rarak*, and *S. delavayi*, it is well demonstrated that the species responses to climate change vary with species and regions (Lindner et al., 2014).

4.3 Risks to *S. mukorossi*, *S. delavayi*, and *S. rarak* under future climate change

Whether a species benefits or suffers under anthropogenic climate change depends on geographical location, ecological niches, and the migration ability of the species, which provide essential insights for spatial conservation assessments of future biodiversity hotspots. In the face of rapid climate change, it is unrealistic for plants to evolve in correlation with physiological adaptation strategies in short periods; therefore, migration or dispersal ability is a prerequisite for their survival (Richard T Corlett, 2009; Liao et al., 2020). This study found that *S. mukorossi*, *S. delavayi*, and *S. rarak* exhibited varying degrees of expansion under future climate change scenarios, especially in *S. delavayi* (Fig. 7). However, we doubt that these species will be able to migrate and spread smoothly into suitable habitats within 100 years. Corlett (Richard T Corlett, 2009) stated that most plants in tropical east Asia may have a maximum dispersal distance in the 100–1000 m range. Engler (R. Engler et al., 2009) stated that unlimited long-distance migration was unrealistic for many mountain plant species. We are not optimistic about the migratory ability of *Sapindus* as a tree species with relatively long generation times, large seeds, and seed dispersal over long distances largely dependent on birds and rodents (J. Liu et al., 2019; J. Liu et al., 2017; Sun et al., 2016). Moreover, if the climate changes dramatically in the future, such as in the SSP370 and SSP585 scenarios, *Sapindus* would be unable to evolve physiological and biochemical traits that are compatible with such scenarios, and would be unable to migrate successfully in a short period of time, and a contraction of suitable habitat areas will be a real possibility.

Consequently, habitats that are likely to contract under future climate change should be prioritised for survey collection of germplasms (J. Liu et al., 2019; Sun et al., 2016; Sun, Wang, et al., 2017), and core germplasms should be ex situ-conserved by vegetative propagation in order to protect as much genetic diversity as possible. In this case, the contraction areas of *S. mukorossi* (Chongqing, Guangxi Zhuang Autonomous Region, Fujian Province, and Hunan Province in China), *S. delavayi* (the periphery of the Sichuan basin and localized of Tibet in China), and *S. rarak* (northern Yunnan province in China, eastern Myanmar, Thailand, Cambodia, Malaysia, Indonesia and the Philippines) should be subjected to germplasm collection and ex situ conservation as soon as possible.

In contrast, Guangdong province, Guangxi Zhuang Autonomous Region, Fujian Province, Hainan Province, and Taiwan in China, which will be relatively less affected by climate change, could be used as a base for resource conservation, breeding, large-scale cultivation, and utilisation of *S. mukorossi* in the future. The Sichuan Basin, Kunming, and Qujing City in the Yunnan Province, China can serve as a base for *S. delavayi*, and the Yunnan Province, China, eastern Myanmar, northern Thailand, and northern Laos can be used as a base for *S. rarak*.

4.4 Uncertainties

In this study, we have likely developed the largest compilation of occurrence records (2041 in total) for *S. mukorossi, S. delavayi*, and *S. rarak* to date; however, the sample size is still relatively small compared to the large study area. Moreover, although climatic, soil, topographical, and solar radiation factors were considered in this model, species habitats are also constrained by other factors, including migration ability, adaptive capacity, inter-species interactions, human activities, and land use. Therefore, the actual habitat distributions of *S. mukorossi, S. delavayi*, and *S. rarak* may be smaller than our model-predicted potential habitat distributions. However, introducing all variables into the model may lead to more collinearity problems, and the effects of key variables may be weakened; thus, the model results may not be more accurate than the current model are. Nevertheless, the modelled current habitat distributions of the three *Sapindus* species investigated in this study matched well with current observations of *Sapindus* distribution patterns (J. Liu et al., 2019; Sun et al., 2018) and accurately reflected the ecological adaptation differences among these three species. We are confident that the MaxEnt model used in this study correctly predicted the potential habitat distribution of these three *Sapindus* species within the context of climate change. We also believe that our results provide an important theoretical basis and recommendations for the conservation and sustainable exploitation of *Sapindus* genetic diversity.

5. Conclusions

We first demonstrated that there were significantly different ecological adaptations among *S. mukorossi*, *S. delavayi*, and *S. rarak* in east and southeast Asia. Climate niche models showed that precipitation may play an important role in framing the potential habitats of *Sapindus*; however, there were significant ecological adaptive divergences among them. *S. mukorossi* exhibited the widest range of adaptation. Compared to that of *S. mukorossi*, *S. delavayi* was more sensitive to minimum temperatures and elevation, and *S. rarak* was more demanding in terms of solar radiation. Under the current environment, *S. mukorossi* displayed the widest distribution of suitable habitats (250.24×10^4 km^2), followed by that of *S. rarak* (173.49×10^4 km^2), while the suitable habitat areas of *S. delavayi* (78.85×10^4 km^2) were only concentrated in the high altitude areas of southwest China.

Under future climate change scenarios, *S. mukorossi*, *S. delavayi*, and *S. rarak* exhibited dramatically divergent responses. The habitat distribution of *S. mukorossi* was predicted to expand and contract under future climate change, with a trend towards expansion at higher latitudes and contraction at lower latitudes. Unlike *S. mukorossi*, a large number of currently unsuitable areas in the Sichuan Basin and Yunnan Province, China will potentially become suitable for *S. delavayi*. In contrast, *S. rarak* exhibited a significant contraction trend, predominantly in the northern Yunnan Province in China, eastern Myanmar, Thailand, Cambodia, Malaysia, Indonesia, and the Philippines. However, we are not optimistic about the migratory ability of *Sapindus*. Therefore, it is recommended that the contraction areas of *S. mukorossi* (Chongqing, Guangxi Zhuang Autonomous Region, Fujian Province, and Hunan Province in China), *S. delavayi* (the periphery of the Sichuan Basin and Tibet in China), and *S. rarak* (northern Yunnan province in China, eastern Myanmar, Thailand, Cambodia, Malaysia, Indonesia, and the Philippines) should be subject to germplasm collection and ex situ conservation. The unchanged areas of suitable habitat under future climate change in the Guangdong province, Guangxi Zhuang Autonomous Region, Fujian Province, Hainan Province, and Taiwan in China, can be used as bases for the conservation, breeding, cultivation, and utilisation of *S. mukorossi* in the future. The unchanged areas of suitable habitat for *S. delavayi* in the Sichuan Basin, Kunming, and Qujing city in the Yunnan Province in China should be used for *S. delavayi* conservation. The unchanged areas of suitable habitat for *S. rarak* in the Yunnan Province in China, eastern Myanmar, northern Thailand, and northern Laos should be used for *S. rarak* conservation.

Declarations

Ethics approval and consent to participate

Not applicable.

Consent for publication

Not applicable.

Competing interests

The authors declare that they have no competing interests

Availability of data and materials

The datasets generated during and/or analysed during the current study are available in the Chinese National Plant Specimen Resource Center, Global Biodiversity Information Facility, Chinese National Specimen Information Infrastructure, WorldClim, Centre for Sustainability and the Global Environment, glUV repository.

Funding

This work was supported by Special Foundation for National Science and Technology Basic Research Program of China (No. 2019FY100803) and “the Fundamental Research Funds for the Central Universities” (2019YC19).

Author Contributions

JML and YYX contributed equally to this work. JML and YYX proposed the idea and completed manuscript. CWS and XW proposed modifications to the methodology and visualisation. XHW, YLZ and SLS collected the data. QYH presented the method and analysed the data. ZC and LMJ improved the manuscript. All authors discussed the results and reviewed the manuscript.

Acknowledgements

We acknowledge the World Climate Research Programme, which, through its Working Group on Coupled Modelling, coordinated and promoted CMIP6. We thank the climate modeling groups for producing and making available their model output, the Earth System Grid Federation (ESGF) for archiving the data and providing access, and the multiple funding agencies who support CMIP6 and ESGF.

References

1. Araujo MB, Pearson RG, Thuiller W, Erhard M (2005) Validation of species–climate impact models under climate change. Glob Change Biol 11(9):1504–1513. https://doi.org/10.1111/j.1365-2486.2005.01000.x
2. Araújo MB, Peterson AT (2012) Uses and misuses of bioclimatic envelope modeling. Ecology, 93(7). https://doi.org/10.1890/11-1930.1
3. Ardestani EG, Mokhtari A (2020) Modeling the lumpy skin disease risk probability in central Zagros Mountains of Iran. Prev Vet Med 176:104887–104887. https://doi.org/10.1016/j.prevetmed.2020.104887
4. Barry C, Moore, Cox PD (1980) Biogeography: An Ecological and Evolutionary Approach: Blackwell. https://doi.org/10.1086/628353
5. Basu A, Basu S, Bandyopadhyay S, Chowdhury R (2015) Optimization of evaporative extraction of natural emulsifier cum surfactant from Sapindus mukorossi—Characterization and cost analysis. Industrial Crops Products 77:920–931. https://doi.org/10.1016/j.indcrop.2015.10.006
6. Beckmann M, Václavík T, Manceur AM, Šprtová L, Wehrden Hv, Welk E, Cord AF (2014) glUV: a global UV-B radiation data set for macroecological studies. Methods in Ecology and Evolution. https://doi.org/10.1111/2041-210X.12168
7. Brown JL (2014) SDMtoolbox: a python-based GIS toolkit for landscape genetic, biogeographic and species distribution model analyses. Methods in Ecology and Evolution. https://doi.org/10.1111/2041-210X.12200
8. Cai G, Xiong H, Jia W, Hu P, Deng L, Wang L,.. . Liu H (2018) The Variation Analysis of the Fruit's Economic and Yield Character of the Sapindus delavayi. Journal of Southwest Forestry University 038(004):37–45. https://doi.org/10.11929/j.issn.2095-1914.2018.04.006
9. Chakraborty M, Baruah DC (2013) Production and characterization of biodiesel obtained from Sapindus mukorossi kernel oil. Energy 60(oct.1):159–167. https://doi.org/10.1016/j.energy.2013.07.065
10. Clark, & D., A (2004) Sources or sinks? The responses of tropical forests to current and future climate and atmospheric composition. Philosophical Transactions of the Royal Society B: Biological Sciences 359(1443):477–491. https://doi.org/10.1007/s00769-002-0536-1
11. Conover WJ (1980) Practical Nonparametric Statistics. Technometrics, 23(4)
12. Convertino M, Annis A, Nardi F (2019) Information-theoretic portfolio decision model for optimal flood management. Environ Model Softw 119:258–274. https://doi.org/10.1016/j.envsoft.2019.06.013
13. Corlett RT (2009) Seed dispersal distances and plant migration potential in tropical East Asia. Biotropica 41(5):592–598. https://doi.org/10.1111/j.1744-7429.2009.00503.x
14. Corlett RT, Westcott DA (2013) Will plant movements keep up with climate change? Trends. in Ecology Evolution 28(8):482–488. https://doi.org/10.1016/j.tree.2013.04.003
15. Eastman J, Florencia S, Elia M, John R, Assaf A (2013) Global Trends in Seasonality of Normalized Difference Vegetation Index (NDVI), 1982–2011. Remote Sensing 5(10):4799–4818. https://doi.org/10.3390/rs5104799
16. Elith J, Graham CH, Anderson RP, Dudik M, Ferrier S, Guisan A,.. . Lehmann A (2006) Novel methods improve prediction of species' distributions from occurrence data. Ecography 29(2):129–151. https://doi.org/10.1111/j.2006.0906-7590.04596.x
17. Elith J, Leathwick JR (2009) Species Distribution Models: Ecological Explanation and Prediction Across Space and Time. Annual Review of Ecology Evolution Systematics 40(1):677–697. https://doi.org/10.1146/annurev.ecolsys.110308.120159
18. Elith J, Phillips SJ, Hastie T, Dudík M, Chee YE, Yates CJ (2011) A statistical explanation of MaxEnt for ecologists. Diversity Distributions, 17(1). https://doi.org/10.1111/j.1472-4642.2010.00725.x
19. Engler A, Melchior H, Werdermann E (1989) A. Engler's Syllabus der Pflanzenfamilien
20. Engler R, Randin CF, Vittoz P, Czáka T, Beniston M, Zimmermann NE, Guisan A (2009) Predicting future distributions of mountain plants under climate change: does dispersal capacity matter? Ecography 32(1):34–45. https://doi.org/10.1111/j.1600-0587.2009.05789.x
21. Gao S, Pan Y, Zhang Q (1991) The effect problem of greenhouse effect on future agriclimatic resoures. Chinese Journal of Agrometeorology 12(04):40549–40405
22. Guisan A, Thuiller W (2005) Predicting species distribution: offering more than simple habitat models. Ecol Lett, 8(9). https://doi.org/10.1111/j.1461-0248.2005.00792.x
23. Guo Y, Guo J, Shen X, Wang G, Wang T (2019) Predicting the Bioclimatic Habitat Suitability of Ginkgo biloba L. in China with Field-Test Validations. Forests, 10(8). https://doi.org/10.3390/f10080705
24. Hanafi-Bojd AA, Vatandoost H, Yaghoobi-Ershadi MR (2020) Climate Change and the Risk of Malaria Transmission in Iran. J Med Entomol 57(1):50–64. https://doi.org/10.1093/jme/tjz131
25. Hatfield JL, Prueger JH (2015) Temperature extremes: Effect on plant growth and development. Weather Climate Extremes 10(PA):4–10. https://doi.org/10.1016/j.wace.2015.08.001
26. He X, Ning X, Guo Y, Wei H (2019) Geographical distribution of Xanthoceras sorbifolia Bunge in China and predicting suitable area under the climate change scenario. Research of Agricultural Modernization, 40(2), 138–146. https://doi.org/CNKI:SUN:NXDH.0.2019-02-016
27. Hewitt G (2000) The genetic legacy of the Quaternary ice ages. Nature. https://doi.org/10.1038/35016000

28. Hu XG, Wang T, Liu SS, Jiao SQ, Jia KH, Zhou SS,.. . Mao JF (2017) Predicting Future Seed Sourcing of Platycladus orientalis (L.) for Future Climates Using Climate Niche Models. Forests, 2017,8(12)(-), -. https://doi.org/10.3390/f8120471
29. Huang Z, Xie L, Wang H, Zhong J, Li Y, Liu J,.. . Huang H (2019) Geographic distribution and impacts of climate change on the suitable habitats of Zingiber species in China. Ind Crops Prod 138:111429. https://doi.org/10.1016/j.indcrop.2019.05.078
30. Jayasinghe SL, Kumar L (2019) Modeling the climate suitability of tea [Camellia sinensis(L.) O. Kuntze] in Sri Lanka in response to current and future climate change scenarios. Agric For Meteorol, 272–273, 102–117. https://doi.org/10.1016/j.agrformet.2019.03.025
31. Kamalesh, Singh, Mahar, and, Tikam, Singh,.. . Anand (2011) Genetic variability and population structure in Sapindus emarginatus Vahl from India. Gene. https://doi.org/10.1016/j.gene.2011.05.036
32. Lawler JJ (2009) Climate Change Adaptation Strategies for Resource Management and Conservation Planning. Ann N Y Acad Sci 1162:79–98. https://doi.org/10.1111/j.1749-6632.2009.04147.x
33. Li G, Du S, Wen Z (2016) Mapping the climatic suitable habitat of oriental arborvitae (Platycladus orientalis) for introduction and cultivation at a global scale. Sci Rep 6:30009. https://doi.org/10.1038/srep30009
34. Liao Z, Zhang L, Nobis MP, Wu X, Pan K, Wang K,.. . Pandey B (2020) Climate change jointly with migration ability affect future range shifts of dominant fir species in Southwest China. Divers Distrib 26(3):352–367. https://doi.org/10.1111/ddi.13018
35. Lindner M, Fitzgerald JB, Zimmermann NE, Reyer C, Delzon S, van der Maaten E,.. . Hanewinkel M (2014) Climate change and European forests: What do we know, what are the uncertainties, and what are the implications for forest management? J Environ Manage 146:69–83. https://doi.org/10.1016/j.jenvman.2014.07.030
36. Liu J, Chen Z, Sun C, Wang L, He Q, Dai T,.. . Weng X (2019) Variation in Fruit and Seed Properties and Comprehensive Assessment of Germplasm Resources of the Genus Sapindus. Sci Silva Sin, 55(6), 44–54. https://doi.org/ CNKI:SUN:LYKE.0.2019-06-006
37. Liu J, Sun C, He Q, Jia LM, Weng XH, Yu J (2017) Research Progress in Sapindus L. Germplasm Resources. World Forest Res v 30(06):15–21. https://doi.org/10.13348/j.cnki.sjlyyj.2017.0071.y
38. Liu Y, Yan L, Li S, Motesharrei S (2015) Spatial and Temporal Patterns of Global NDVI Trends: Correlations with Climate and Human Factors. Remote Sensing 7(10):13233–13250. https://doi.org/10.3390/rs71013233
39. Mahar KS, Meena B, Rana TS, Ranade SA (2011) ISSR analysis of soap nut (Sapindus mukorossi Gaertn.) genotypes in Western Himalaya (India). Giornale Botanico Italiano 146(3):614–621. https://doi.org/10.1080/11263504.2011.637090
40. Mahar KS, Rana TS, Ranade SA, Pande V, Palni LMS (2013) Estimation of genetic variability and population structure in Sapindus trifoliatus L., using DNA fingerprinting methods. Trees 27(1):85–96. https://doi.org/10.1007/s00468-012-0770-z
41. Melo-Merino SM, Reyes-Bonilla H, Lira-Noriega A (2020) Ecological niche models and species distribution models in marine environments: A literature review and spatial analysis of evidence. Ecol Model, 415. https://doi.org/10.1016/j.ecolmodel.2019.108837
42. Merow C, Smith MJ, Edwards TC, Guisan A, Mcmahon SM, Normand S,.. . Elith J (2014) What do we gain from simplicity versus complexity in species distribution models? Ecography 37(12):1267–1281. https://doi.org/10.1111/ecog.00845
43. Merow C, Smith MJ, Silander JA (2013) A practical guide to MaxEnt for modeling species' distributions: what it does, and why inputs and settings matter. Ecography, 36. https://doi.org/10.1111/j.1600-0587.2013.07872.x
44. Mukherjee S, Mukhopadhyay S, Pariatamby A, Hashim MA, Redzwan G, Gupta BS (2015) Optimization of pulp fibre removal by flotation using colloidal gas aphrons generated from a natural surfactant. J Taiwan Inst Chem Eng 53:15–21. https://doi.org/10.1016/j.jtice.2015.02.037
45. Mukhopadhyay S, Hashim MA, Sahu JN, Yusoff I, Gupta BS (2013) Comparison of a plant based natural surfactant with SDS for washing of As(V) from Fe rich soil. J Environ Sci, 25(11). https://doi.org/10.1016/S1001-0742(12)60295-2
46. Mukhopadhyay S, Mukherjee S, Adnan NF, Hayyan A, Hayyan M, Hashim MA, Gupta S, B (2016) Ammonium-based deep eutectic solvents as novel soil washing agent for lead removal. Chem Eng J 294:316–322. https://doi.org/10.1016/j.cej.2016.02.030
47. Muntaha ST, Khan MN (2015) Natural surfactant extracted from Sapindus mukurossi as an eco-friendly alternate to synthetic surfactant - a dye surfactant interaction study. J Clean Prod 93(apr.15):145–150. https://doi.org/10.1016/j.jclepro.2015.01.023
48. Neukom R, Barboza LA, Erb MP, Feng S, Gunten LV (2019) Consistent multidecadal variability in global temperature reconstructions and simulations over the Common Era. Nat Geosci, 12(8). https://doi.org/10.1038/s41561-019-0400-0
49. Pal AK, Vaishnav V, Meena B, Pandey N, Singh T (2020) The adaptive fitness of Sapindus emarginatus Vahl populations towards future climatic regimes and the limiting factors of its distribution. Sci Rep. https://doi.org/10.1038/s41598-020-60219-8
50. Pea RDL, Hughes JD (2007) Improving vegetable productivity in a variable and changing climate. International Crops Research Institute for the Semi-Arid Tropics. https://doi.org/10.1002/etc.5620080106
51. Pelegrini BL, Sudati EA, Re F, Moreira AL, Ferreira P, Sampaio IC, de Souza Lima AR, M. M (2017) Thermal and rheological properties of soapberry Sapindus saponaria L. (Sapindaceae) oil biodiesel and its blends with petrodiesel. Fuel 199(JUL.1):627–640. https://doi.org/10.1016/j.fuel.2017.02.059
52. Peng L-P, Cheng F-Y, Hu X-G, Mao J-F, Xu X-X, Zhong Y,.. . Xian H-L (2019) Modelling environmentally suitable areas for the potential introduction and cultivation of the emerging oil crop Paeonia ostii in China. Sci Rep, 9. https://doi.org/10.1038/s41598-019-39449-y
53. Phillips SJ (2008) Transferability, sample selection bias and background data in presence-only modelling: a response to Peterson et al. (2007). Ecography, 31(2), 272–278. https://doi.org/10.1111/j.0906-7590.2008.5378.x
54. Phillips SJ, Anderson RP, Schapire RE (2006) Maximum entropy modeling of species geographic distributions. Ecol Model. https://doi.org/10.1016/j.ecolmodel.2005.03.026

55. Prevéy JS, Parker LE, Harrington CA, Lamb CT, Proctor MF (2020) Climate change shifts in habitat suitability and phenology of huckleberry (Vaccinium membranaceum). Agric For Meteorol, 280. https://doi.org/10.1016/j.agrformet.2019.107803
56. Ramos RS, Kumar L, Shabani F, Picanco MC (2019) Risk of spread of tomato yellow leaf curl virus (TYLCV) in tomato crops under various climate change scenarios. Agric Syst 173:524–535. https://doi.org/10.1016/j.agsy.2019.03.020
57. Ray R, Gururaja KV, Ramchandra TV (2011) Predictive distribution modeling for rare Himalayan medicinal plant Berberis aristata DC. J Environ Biol 32(6):725–730. https://doi.org/10.1007/s11367-011-0315-5
58. Rodriguez-Hernández D, Demuner AJ, Barbosa LCA, Csuk R, Heller L (2015) Hederagenin as a triterpene template for the development of new antitumor compounds. Eur J Med Chem 105:57–62. https://doi.org/10.1016/j.ejmech.2015.10.006
59. Rong Z, Zhao C, Liu J, Gao Y, Zang F, Guo Z,.. . Wang L (2019) Modeling the Effect of Climate Change on the Potential Distribution of Qinghai Spruce (Picea crassifolia Kom.) in Qilian Mountains. Forests, 10(1). https://doi.org/10.3390/f10010062
60. Shinobu-Mesquita C, Bonfim-Mendon?A P, Moreira A, Ferreira I, Donatti L, Fiorini A, Svidzinski T (2015) Cellular Structural Changes in Candida albicans Caused by the Hydroalcoholic Extract from Sapindus saponaria L. Molecules 20(5):9405–9418. https://doi.org/10.3390/f10010062
61. Singh PTD, Singh MM (2008) Anti-Trichomonas activity of Sapindus saponins, a candidate for development as microbicidal contraceptive. J Antimicrob Chemother 62(3):526–534. https://doi.org/10.1093/jac/dkn223
62. Smułek W, Zdarta A, łuczak M, Krawczyk P, Jesionowski T, Kaczorek E (2016) Sapindus saponins' impact on hydrocarbon biodegradation by bacteria strains after short- and long-term contact with pollutant. Colloids Surfaces B Biointerfaces 142:207–213. https://doi.org/10.1016/j.colsurfb.2016.02.049
63. Sterne TK, Retchless D, Allee R, Highfield W (2020) Predictive modelling of mesophotic habitats in the north-western Gulf of Mexico. Aquatic Conservation-Marine and Freshwater Ecosystems. https://doi.org/10.1002/aqc.3281
64. Stocker TF, Qin D, Plattner GK, Tignor M, Allen SK, Boschung J,.. . Midgley BM (2013) IPCC, 2013: Climate Change 2013: The Physical Science Basis. Contribution of Working Group I to the Fifth Assessment Report of the Intergovernmental Panel on Climate Change. Computational Geometry 18(2):95–123. https://doi.org/10.1017/CBO9781107415324
65. Stocker TF, Qin D, Plattner GK, Tignor MMB, Allen SK, Boschung J,.. . Midgley PM (2014) Climate Change 2013: The Physical Science Basis. Contribution of Working Group I to the Fifth Assessment Report of IPCC the Intergovernmental Panel on Climate Change. http://www.ipcc.ch/publications_and_data/publications_ipcc_fourth_assessment_report_wg1_report_the_physical_science_basis.htm, 18(2), 95–123
66. Sultana S, Baumgartner JB, Dominiak BC, Royer JE, Beaumont LJ (2020) Impacts of climate change on high priority fruit fly species in Australia. Plos One, 15(2). https://doi.org/10.1371/journal.pone.0213820
67. Sun C, Jia L, Xi B, Liu J, Wang L, Weng X (2019) Genetic diversity and association analyses of fruit traits with microsatellite ISSRs in Sapindus. Journal of Forestry Research 030(001):193–203. https://doi.org/10.1007/s11676-017-0580-7
68. Sun C, Jia L, Xi B, Wang L, Weng X (2017) Natural variation in fatty acid composition of Sapindus spp. seed oils. Industrial Crops Products 102:97–104. https://doi.org/10.1016/j.indcrop.2017.03.011
69. Sun C, Jia L, Ye Ho, Gao Y, Weng X (2016) Geographic variation evaluating and correlation with fatty acid composition of economic characters of Sapindus spp. Fruits Journal of Beijing Forestry University 12:73–83. https://doi.org/10.13332/j.1000-1522.20160143
70. Sun C, Wang J, Duan J, Zhao G, Weng X, Jia L (2017) Association of Fruit and Seed Traits of Sapindus mukorossi Germplasm with Environmental Factors in Southern China. Forests 8(12):491–491. https://doi.org/10.3390/f8120491
71. Sun C, Wang L, Liu J, Zhao G, Gao S, Xi B,.. . Jia L (2018) Genetic structure and biogeographic divergence among Sapindus species: An inter-simple sequence repeat-based study of germplasms in China. Industrial Crops Products 118:1–10. https://doi.org/10.1016/j.indcrop.2018.03.029
72. Taylor DW (1990) Paleobiogeographic relationships of angiosperms from the Cretaceous and early Tertiary of the North American area. Bot Rev, 56(4). 10.1007/BF02995927
73. Thomas CD, Cameron A, Green RE, Bakkenes M, Beaumont LJ, Collingham YC,.. . Hannah L (2003) Extinction risk from climate change. Nature 427:145–148. https://doi.org/10.1038/nature02121
74. Tran D, Vien (2011) Climate change and its impact on agriculture in Vietnam. Journal of the International Society for Southeast Asian Agricultural Sciences 17(1):17–21
75. Wang W, Yang J, Luo X, Zhou C, Chen S, Yang Z,.. . Li Y (2019) Assessment of Potential Habitat for Firmiana danxiaensis, a Plant Species with Extremely Small Populations in Danxiashan National Nature Reserve Based on Maxent Model. Scientia Silvae Sinicae(8). https://doi.org/CNKI:SUN:LYKE.0.2019-08-003
76. Wang X, Liu J, Rui X, Xu Y, Jia L (2020) Biogeographic divergence in leaf traits of Sapindus mukorossi and Sapindus delavayi and its relation to climate. Journal of Forestry Research(4), 1–12. https://doi.org/10.1007/s11676-020-01206-7
77. Xia N (1995) Geographical distribution of Sapindaceae in China. Journal of Tropical Subtropical Botany 000(001):13. https://doi.org/CNKI:SUN:RYZB.0.1995-01-001
78. Xu Y, Jia L, Chen Z, Gao Y (2018) Advances on Triterpenoid Saponin of Sapindus mukorossi. Chem Bull 081(012):1078–1088
79. Zhang L, Jing Z, Li Z, Liu Y, Fang S (2019) Predictive Modeling of Suitable Habitats for Cinnamomum Camphora (L.) Presl Using Maxent Model under Climate Change in China. International Journal of Environmental Research Public Health, 16(17). https://doi.org/10.3390/ijerph16173185
80. Zhu G, Liu G, Bu W, Gao Y (2013) Ecological niche modeling and its applications in biodiversity conservation. Biodiversity Science(01), 94–102. https://doi.org/10.3724/SP.J.1003.2013.09106

Figures

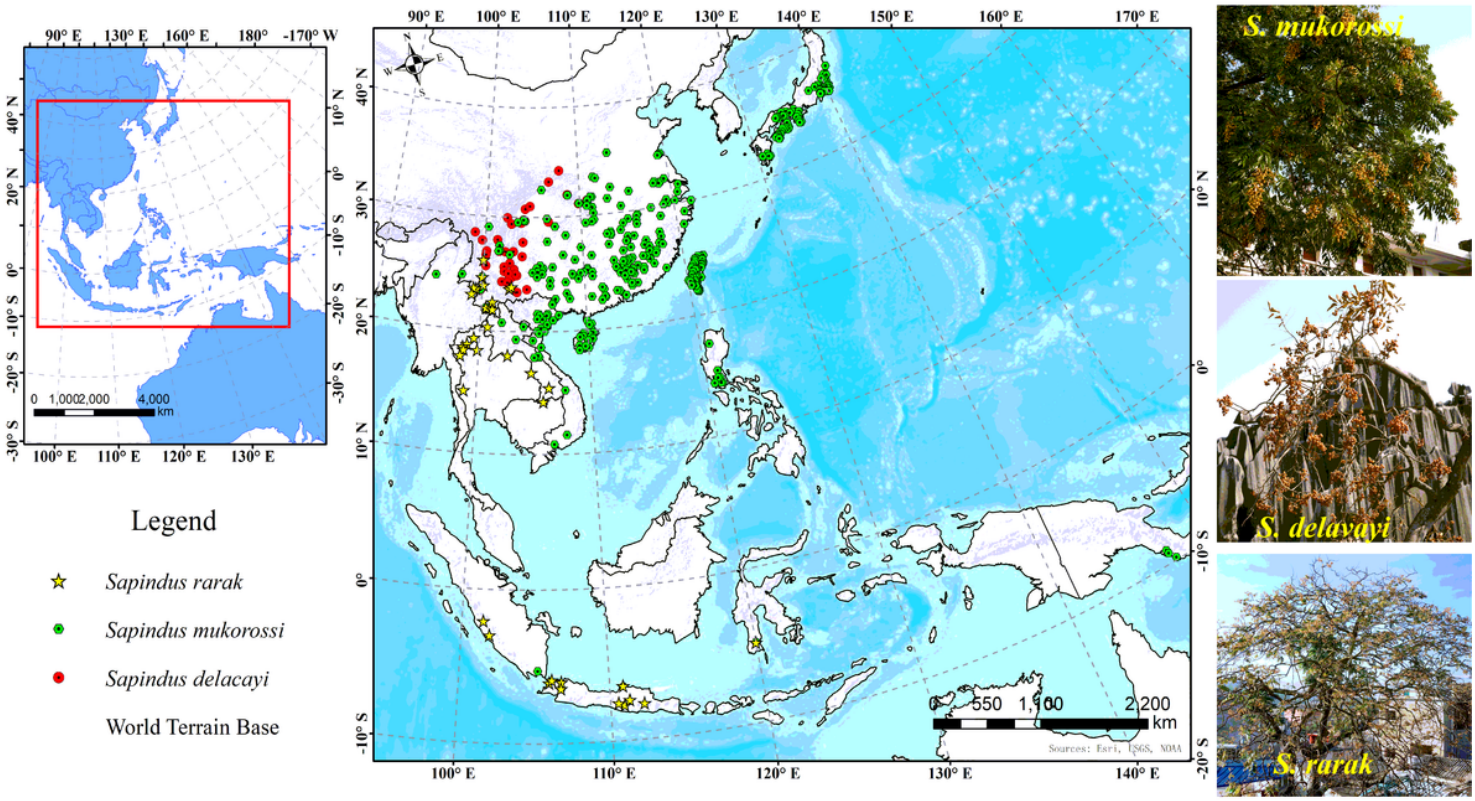

Figure 1

Spatial distribution of occurrence records of S. mukorossi, S. delavayi, and S. rarak. Note: The designations employed and the presentation of the material on this map do not imply the expression of any opinion whatsoever on the part of Research Square concerning the legal status of any country, territory, city or area or of its authorities, or concerning the delimitation of its frontiers or boundaries. This map has been provided by the authors.

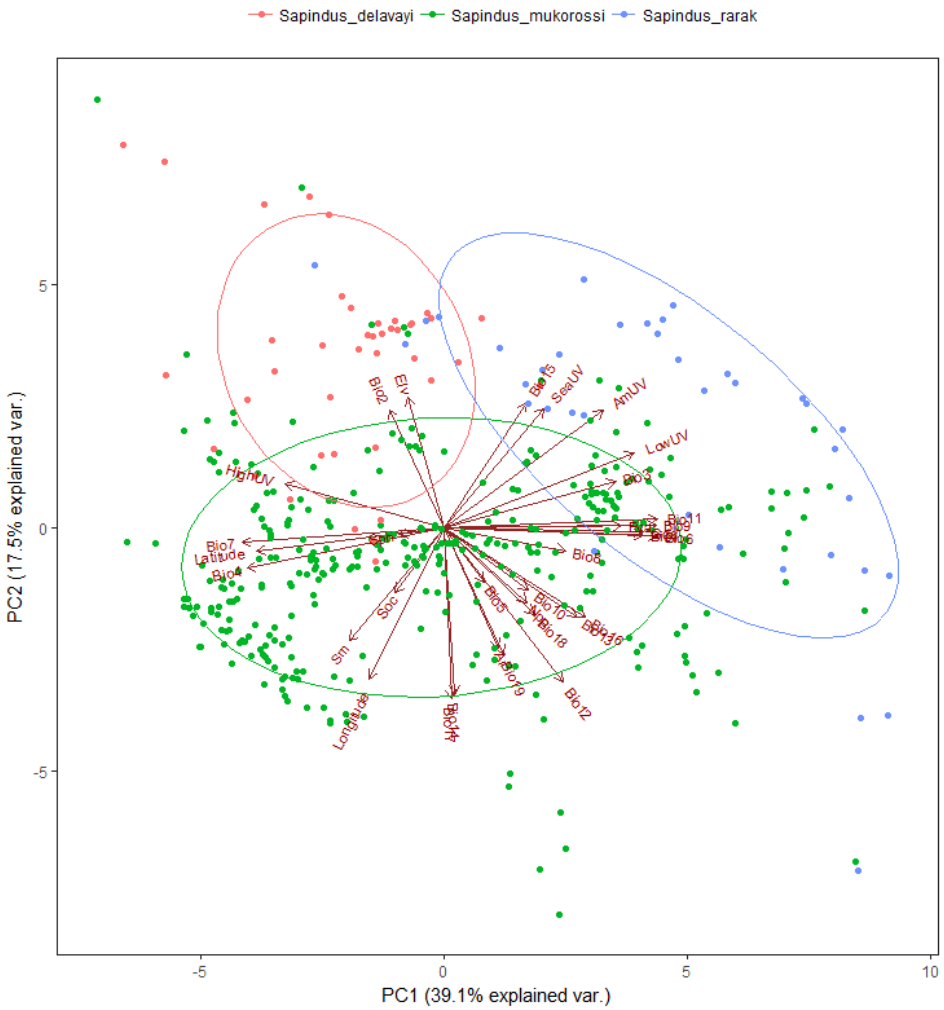

Figure 2

Principal component analysis distance biplot for the 419 occurrences on 33 environmental variables.

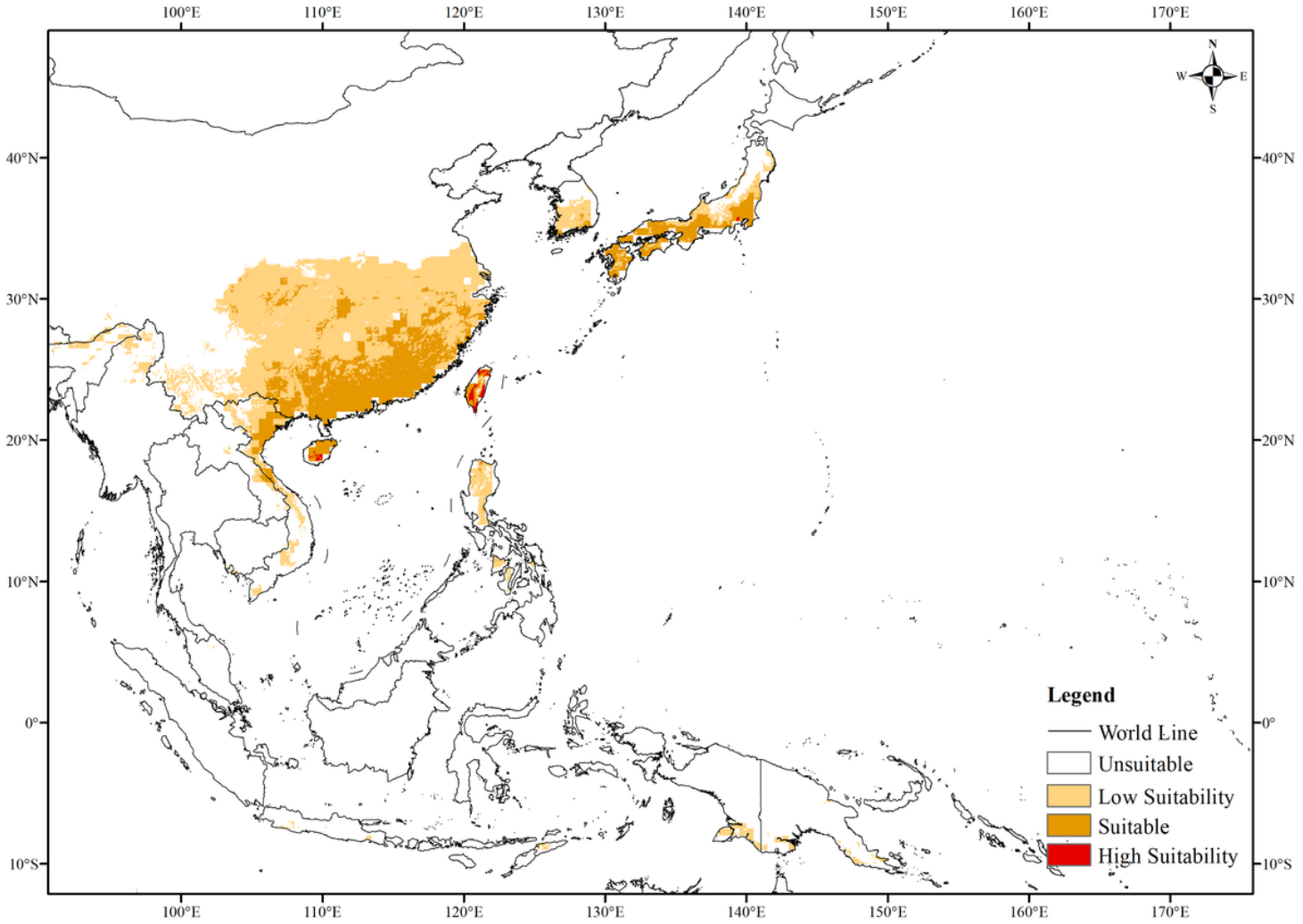

Figure 3

Suitable habitat distribution of S. mukorossi under the current environment. Note: The designations employed and the presentation of the material on this map do not imply the expression of any opinion whatsoever on the part of Research Square concerning the legal status of any country, territory, city or area or of its authorities, or concerning the delimitation of its frontiers or boundaries. This map has been provided by the authors.

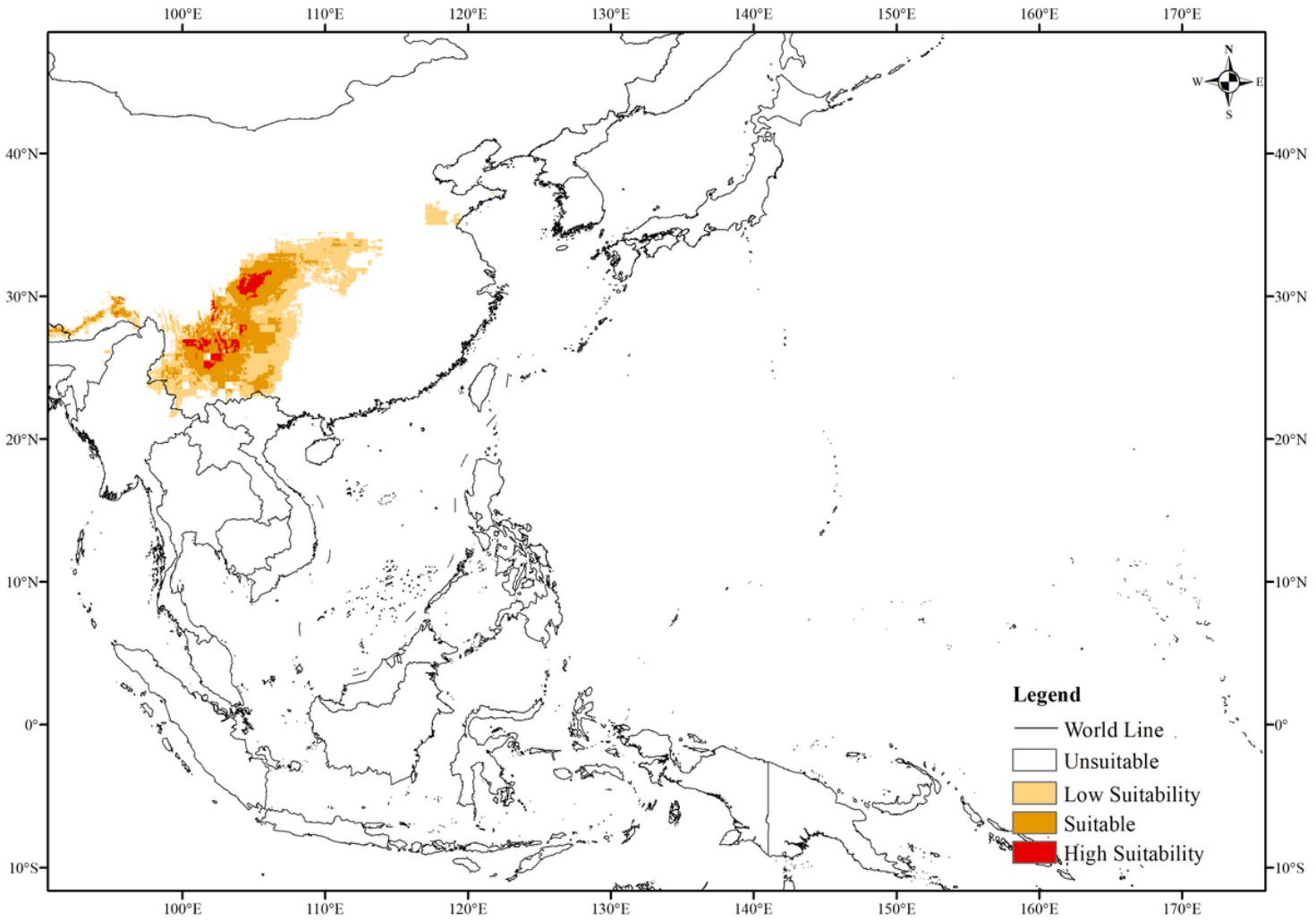

Figure 4

Suitable habitat distribution of S. delavayi under the current environment. Note: The designations employed and the presentation of the material on this map do not imply the expression of any opinion whatsoever on the part of Research Square concerning the legal status of any country, territory, city or area or of its authorities, or concerning the delimitation of its frontiers or boundaries. This map has been provided by the authors.

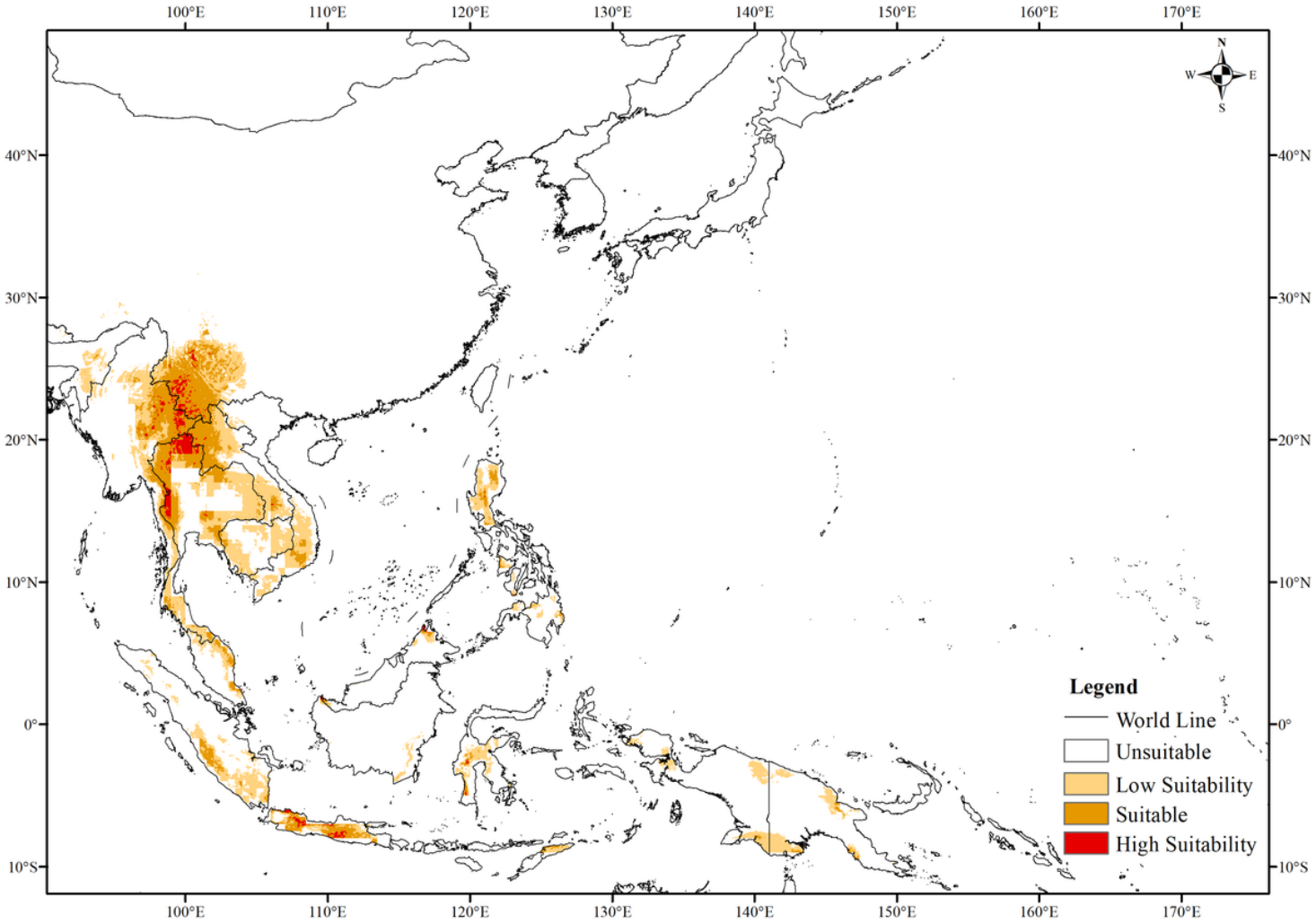

Figure 5

Suitable habitat distribution of S. rarak under the current environment. Note: The designations employed and the presentation of the material on this map do not imply the expression of any opinion whatsoever on the part of Research Square concerning the legal status of any country, territory, city or area or of its authorities, or concerning the delimitation of its frontiers or boundaries. This map has been provided by the authors.

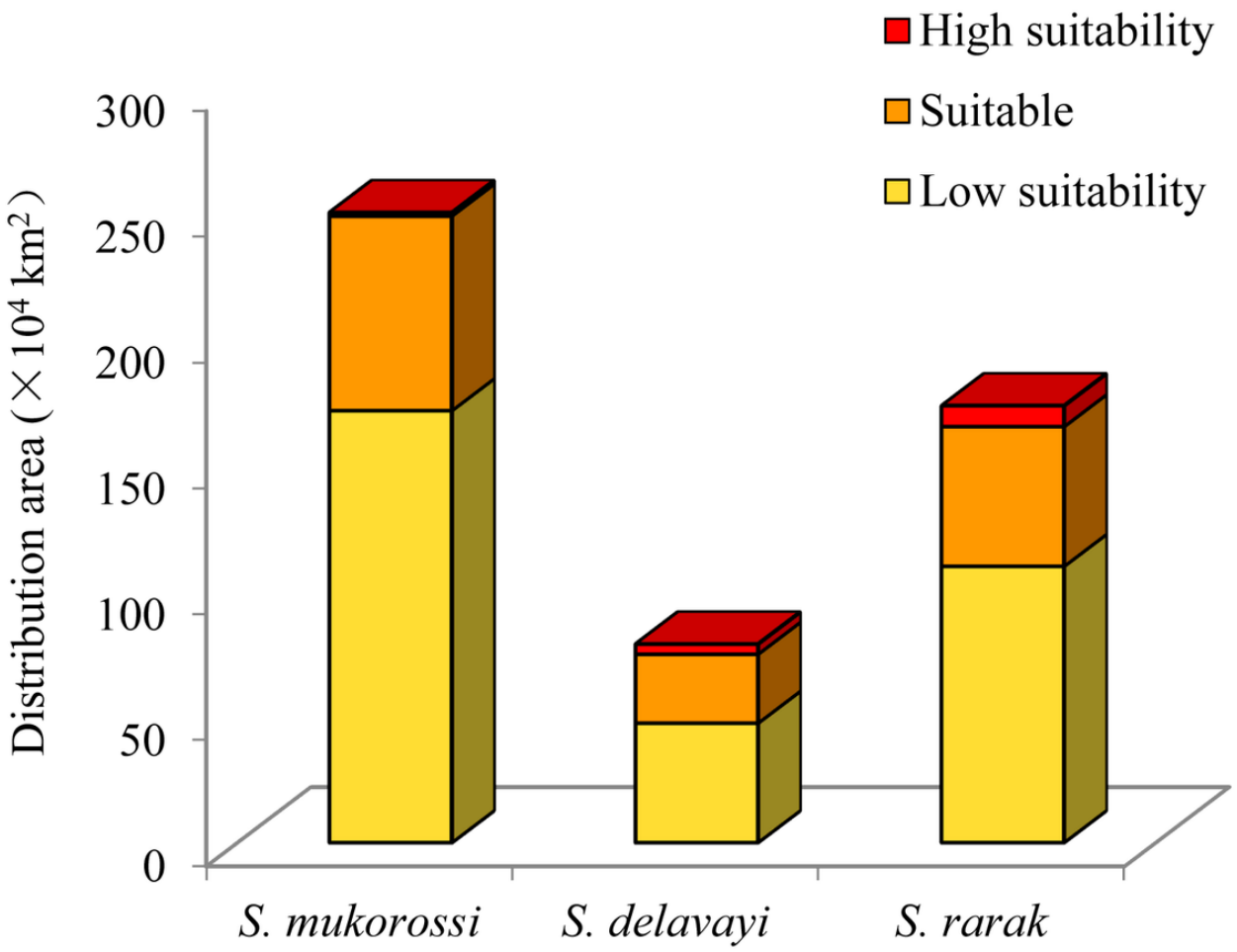

Figure 6

Distribution of suitable habitats areas for S. mukorossi, S. delavayi, and S. rarak under the current environment.

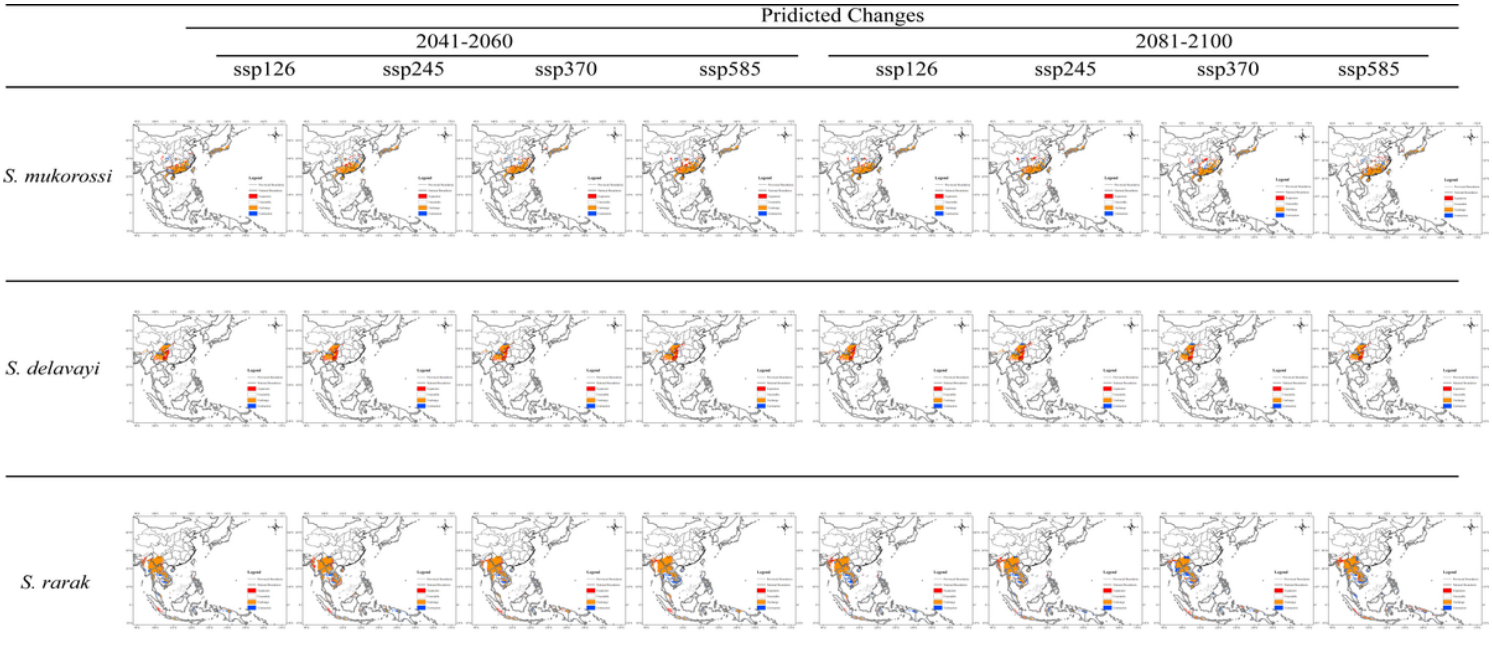

Figure 7

Projected future distributions of the period from 2020–2100 for S. mukorossi, S. delavayi, and S. rarak, and the changes in areas between future and current distributions under four emission scenarios (SSP126, SSP245, SSP370, and SSP585). Note: The designations employed and the presentation of the material on this map do not imply the expression of any opinion whatsoever on the part of Research Square concerning the legal status of any country, territory, city or area or of its authorities, or concerning the delimitation of its frontiers or boundaries. This map has been provided by the authors.

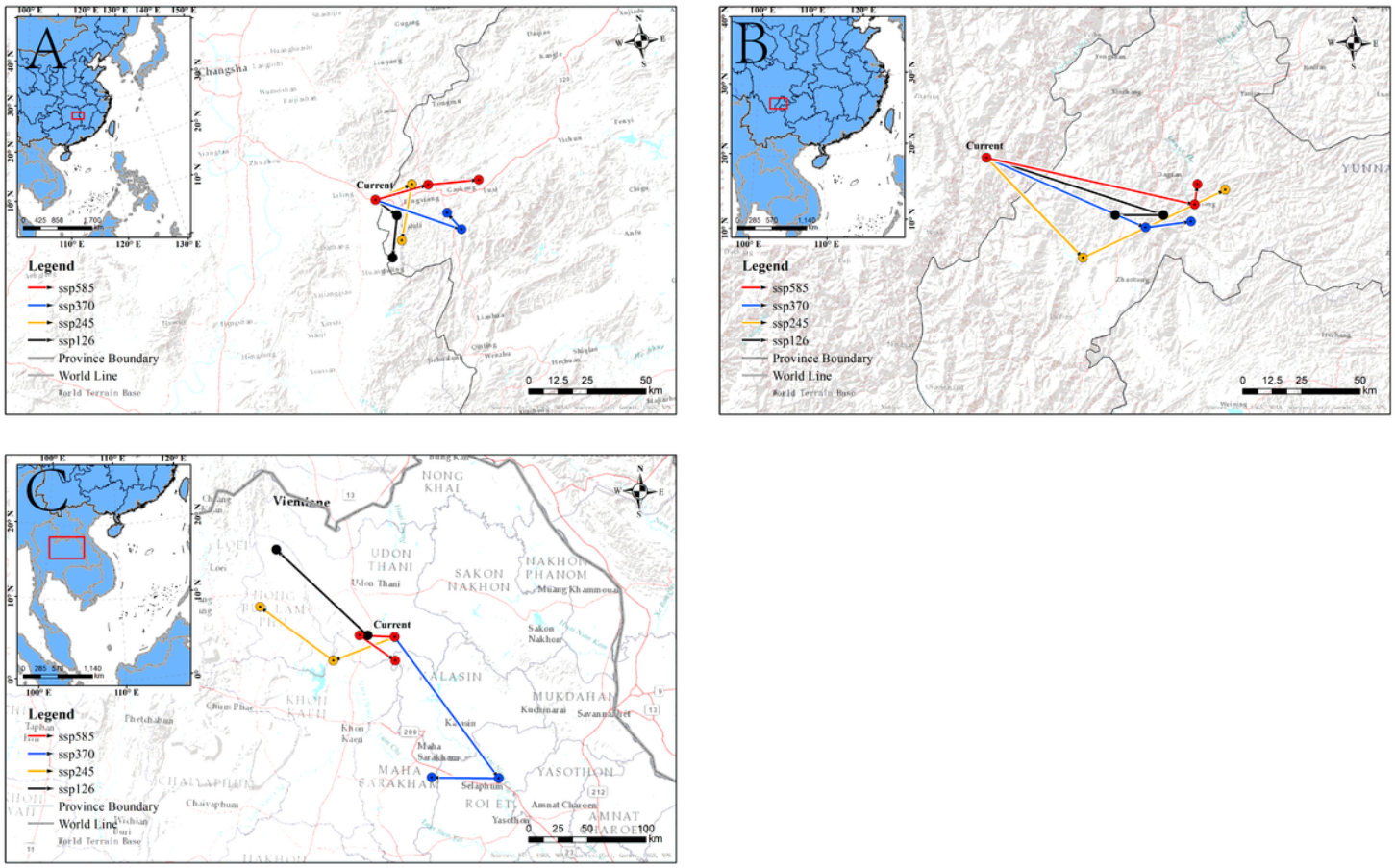

Figure 8

Centroid shifts projected habitat distributions for S. mukorossi, S. delavayi, and S. rarak under four emission scenarios (SSP126, SSP245, SSP370, and SSP585). A): S. mukorossi, B): S. delavayi, C): S. rarak. Note: The designations employed and the presentation of the material on this map do not imply the expression of any opinion whatsoever on the part of Research Square concerning the legal status of any country, territory, city or area or of its authorities, or concerning the delimitation of its frontiers or boundaries. This map has been provided by the authors.

Supplementary Files

This is a list of supplementary files associated with this preprint. Click to download.

- Supplementarydata.docx